ARTICLE

Preparation of TiO_2 Graphene Oxide composites and Its application in coking wastewater treatment

Jiliang Xie [1,*], **Yanxia Zeng**[1] **and Xia Sun**[2]

[1] Institute of marine research development , Jiangsu Ocean University, Lianyungang 222005, Jiangsu, China
[2] School of envirronmental and chemical engineering,jiangsu ocean university, Lianyungang 222005, Jiangsu, China

Abstract

Graphene is a new type of carbon-based material discovered in 2004, composed of a single layer of carbon atoms tightly packed. It has a two-dimensional honeycomb lattice structure. Since carbon atoms in graphene are sp^2 hybridized and generally have a planar two-dimensional structure, its excellent film-forming properties make it a potential application in the field of film materials. At the same time, graphene has also received increasing attention in the field of photocatalysis due to its excellent electron transport ability. In this thesis, we will comprehensively utilize graphene's film-forming properties and photocatalytic enhancement properties to prepare graphene-based composite membrane materials, and study the application of these membranes in the field of wastewater treatment. The main contents are as follows: (1) We use graphene oxide sheets as carriers to support TiO_2 nanoparticles to form graphene oxide-TiO_2 composite sheets. After reassembly, a graphene oxide-TiO_2 composite film is formed. Due to the intercalation of nanoparticles between graphene oxide sheets, the special two-dimensional channels in the obtained composite membrane become larger, improving the permeation performance of the composite membrane. The amount of loaded nanoparticles can be adjusted by changing the amount of graphene oxide and Ti salt, and with an increase in the amount of TiO_2, the permeability of the membrane improves. Due to the low crystallinity of TiO_2 and the poor photocatalytic performance of the composite film itself, we fixed an upper photocatalyst (P25) on the graphene oxide-TiO_2 composite film using a simple filtering method to form a multi-layer filter film. Under light conditions, trapped dye molecules can be quickly decomposed, allowing the filter membrane to have a self-cleaning function. (2)Graphene can not only be assembled to form a graphene membrane but also can be used as a filler for membranes. We assembled TiO_2 nanowires into a filter membrane with a large pore size and added a certain proportion of graphene oxide, allowing graphene oxide sheets to be relatively uniformly dispersed within the filter membrane. Reduced graphene oxide is obtained by reduction. Due to the existence of graphene sheets, in films assembled with TiO_2 nanowires, pores are partially blocked by graphene sheets. At the same time, due to the addition of graphene, the adsorption capacity of the filter membrane is enhanced. The TNW-G complex exhibits photodegradation ability for direct yellow dye solution under UV light irradiation.

Keywords: Graphene, photocatalysis, wastewater treatment, composite membranes, TiO_2

Citation
Jiliang Xie, Yanxia Zeng, and Xia Sun (2024). Preparation of TiO_2 Graphene Oxide composites and Its application in coking wastewater treatment. Mari Papel Y Corrugado, 2024(1), 59–68.

Submitted: 30 August 2024
Accepted: 10 September 2024
Published: 16 November 2024

Vol. 2024, **No.** 1, 2024.

***Corresponding author:**
✉ Jiliang Xie
jiliangxie@jou.edu.cn

1 Introduction

In the early years [1, 2], the concept of single-layer graphite, namely graphene, was proposed, and the electronic properties of graphene were studied using the tight binding model. At the same time, it was

pointed out that a small part of the valence band of graphite extends into the conduction band. Therefore, graphite is a semiconductor without activation energy, and this research has laid a foundation for exploring some physical properties of graphite using solid energy band theory. Since then, research on graphene has remained at the theoretical level for decades [3, 4]. In the laboratory, through mechanical exfoliation, high-quality single-crystal graphite films with similar metallic properties, only one atom thick, were obtained that can exist stably at room temperature. This marked the first successful isolation of graphene. For this achievement, two scientists won the Nobel Prize in Physics. Graphene is a two-dimensional material with a thickness of only one carbon atom. The carbon atoms in graphene are arranged in sp^2 hybrid orbitals, forming a planar film with a hexagonal honeycomb lattice. This two-dimensional graphite material is structured in a hexagonal array like a wire mesh, which can be regarded as a large planar fullerene molecule. Its hardness is ten times that of steel. Furthermore, this film is a two-dimensional semimetal with a small overlap between the valence band and the conduction band, exhibiting a strong second-order electric field effect. The electron concentration can reach 10^{13} cm^{-2}, and the room-temperature mobility induced by applying a gate voltage can reach 10,000 cm^2/Vs, offering excellent conductivity with minimal energy loss. The structure of graphene is shown in Figure 1.

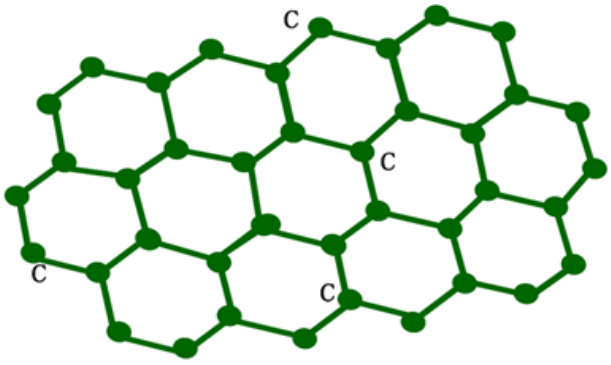

Figure 1. Structure diagram of graphene

Titanium dioxide has the advantages of low cost, non-toxicity, and excellent photocatalytic performance [5, 6]. Therefore, it has attracted considerable attention and research interest. Titanium dioxide, with its unique properties, is the preferred material for combining with graphene. In 1929, it was discovered that titanium dioxide could cause paint to fade due to its photosensitive properties. In 1977, semiconductor materials were utilized in fields such as sterilization and wastewater treatment. Most of the atoms in TiO_2 nanomaterials are located on the surface, giving it a large specific surface area with strong adsorption capacity, high strength, and good ductility. Generally, smaller size corresponds to greater hardness and enhanced diffusion ability [7, 8]. It has a strong absorption effect on high-energy ultraviolet light. Through a series of photochemical reactions, organic matter in water can be degraded to generate non-toxic and harmless carbon dioxide and water [9, 10]. The photocatalytic abilities of different crystalline forms vary, but its chemical stability is generally high, making it a subject of extensive study across various fields.

Coking wastewater refers collectively to high-concentration organic wastewater generated during processes such as coking, gas purification, and coking product recovery. Coking wastewater has the following main characteristics: (1) it contains many types of pollutants with complex components; (2) it has many refractory substances; (3) it is highly toxic; (4) it has poor biodegradability; (5) it has high chromaticity. Currently, coking wastewater treatment methods mainly include activated carbon adsorption, coagulation sedimentation, and biochemical treatment, but the COD value remains difficult to reach the primary discharge standard. Photocatalytic oxidation is a water treatment technology that has emerged in recent decades, representing an advanced oxidation technology that is currently under active research [11, 12]. Photocatalysis refers to the catalytic reaction of a photocatalyst under light irradiation. Given sufficient reaction time, organic pollutants can be completely mineralized into simple inorganic substances such as CO_2 and H_2O through photocatalysis, thereby avoiding secondary environmental pollution. This simple, efficient, and promising wastewater treatment method has been widely studied [13, 14]. Pure TiO_2 has been considered a nearly ideal photocatalyst material due to its stable chemical properties, low cost, non-toxicity, and high activity [5–16]. However, TiO_2 is a semiconductor with a wide band gap, which can only absorb ultraviolet light in sunlight (accounting for only 3-5% of solar energy). Additionally, photogenerated electron-hole pairs in TiO_2 are easily recombined, which greatly limits the photocatalytic efficiency of TiO_2, making the effect of modified TiO_2 photocatalysts less than ideal. Thus, the research and development of high-performance modified TiO_2 photocatalyst materials are necessary. Furthermore, expanding the light absorption range of TiO_2 and

inhibiting the recombination of photogenerated carriers are crucial to improving its photocatalytic performance. Since its discovery, graphene has attracted researchers' attention due to its unique two-dimensional structure, excellent electrical and thermal conductivity, and large specific surface area. Experimental studies on using graphene to modify TiO_2 have gradually emerged. Many theories and practical applications have proven that the insertion of graphene can indeed inhibit the recombination of photogenerated electron-hole pairs in TiO_2, prolong the duration of photocatalytic oxidation and pollutant degradation, and thus improve the photocatalytic performance of TiO_2. However, in many studies, the practical application of photocatalysts to visible light remains relatively underdeveloped.

Although TiO_2 nanowire membranes have promising applications in water treatment, their large pore size, lack of selective separation ability, and low activity present limitations [17, 18]. We improve the filtration performance of TiO_2 nanowire membranes by adding graphene. At the same time, the excellent conductivity of graphene enhances the photocatalytic activity of the TiO_2 semiconductor, thereby improving the photocatalytic self-cleaning ability of TiO_2 nanowire films [19, 20]. Moreover, traditional TiO_2 responds only to ultraviolet light, limiting its application in practical settings. Based on previous research, we have developed a TiO_2 nanowire membrane with selective separation ability and attempted to broaden its light response range, allowing the new composite photocatalyst to use visible light to degrade pollutants and make full use of solar energy resources.

2 Materials and methods

The primary experimental reagents are listed in Table 1, while the main testing instruments are detailed in Table 2.

Name	Specifications
Graphite	325 mesh
Potassium permanganate	AR
Concentrated sulfuric acid	AR
Hydrogen peroxide solution	AR
Hydrochloric acid	AR
Barium sulfate	AR
Titanium sulfate	CP
Sodium hydroxide	AR
Nanometer titanium dioxide	Degussa P25 grade
Direct Red 80	BC
Direct Blue 15	BC
Direct Yellow 50	BC

Table 1. Reagent specifications and manufacturers

2.1 Preparation of membrane

2.1.1 Preparation of graphene oxide (GO)

Pour 230 mL of concentrated sulfuric acid into a dry round-bottom flask (5000 mL), place it in an ice-water bath (0 ℃), and add 10 g of graphite powder while stirring. After mixing evenly, slowly add 30 g of potassium permanganate in portions to maintain the system temperature within 20 ℃. After uniform mixing, place the flask in a 35 ℃ water bath and maintain the temperature for 2 hours, then add 460 mL of deionized water. After 15 minutes of mixing, add 1.4 L of deionized water to terminate the reaction, continue to stir for 5 minutes, and then add 30 mL of 30% hydrogen peroxide. At this point, the reaction solution changes from brown-black to bright yellow. Allow the solution to stand for one day, pour off the upper clear solution, and wash the precipitate with dilute hydrochloric acid (1:10 volume ratio) until there is no SO_4. Dialyze the solution for several days until no Cr ions are detected. Finally, store the obtained graphene oxide in a brown glass bottle for later use.

2.1.2 Preparation of graphene oxide TiO_2 (GOT) film

Disperse 30 mg of $Ti(SO_4)_2$ in 20 mL of graphene oxide dispersion (1 mg/mL) and place the mixture at 60 ℃ for 24 hours. Centrifuge the product with water until neutral. Then, re-disperse the obtained sample in water and adjust the dispersion to a pH value of about 10 with ammonia to form a stable graphene oxide TiO_2 (GOT) dispersion. Prepare the GOT filter membrane by vacuum filtration on a polycarbonate filter membrane (diameter: 47 mm, pore diameter: 0.2 μm) using 0.2 mg of graphene oxide in 30 mL of water.

2.1.3 Preparation of GOT/P25 filter membrane

Further filter a TiO_2 dispersion (10 mL of water containing 1.5 mg of P25 nanoparticles) on the previously obtained GOT membrane to prepare a multilayer filter membrane with a GOT/P25 structure.

2.1.4 Preparation of titanium dioxide nanowires (TNWs)

Pour 40 mL of 10 M NaOH solution into a 50 mL reaction vessel, add 0.2 g of P25, stir for 30 minutes, and place the reactor in an oven at 180 ℃ for 3 days. Wash with 0.2 M HCl solution and deionized water until neutral, and finally disperse the product in deionized water to obtain TNWs for future use.

Instrument	Model	Producer
Vacuum pump	V-700	BUCHI, Switzerland
Temperature controlled agitator	RCT set 1	IKA, Germany
Multi function agitator	ML-902	Shanghai Pudong Analytical Instrument Factory
Ultrasonic cell pulverizer	JY92-IIN	Ningbo Xinzhi Biotechnology Co., Ltd
Ultrasonic cleaner	Kudos SK2200H	Shanghai Kedao Ultrasonic Instrument Co., Ltd
Transmission electron microscope	Tecnai G2 F20 S-TWIN	FEI
X ray powder diffractometer	D8 Advance	Bruker, Germany
Scanning electron microscope	SU8010	HITIACHI, Japan
Full automatic physical and chemical adsorption instrument	ASAP 2020	Micromeritics
Total organic carbon analyzer	TOC-VCPH	Shimadzu Co.
UV Vis spectrophotometer	Cary 50	Varian, USA
Thermogravimetric analyzer	Thermo-gravimetric analyzer	NETZSCH, Germany
Ultraviolet lamp 254mm	TUV 4W T5	Philips, Netherlands
Electronic balance	SARTORIUS AG	Sartorius, Germany

Table 2. Model and Origin of Instrument

2.1.5 Preparation of titanium dioxide nanowire graphene membrane (TNW-G) membrane

Sonicate 2 mg/mL of GO for 1 hour and use the GO dispersion as the graphene raw material to prepare TNW-G membranes with different GO contents. For example, to prepare a TNW-G1% membrane with 1% GO content, place 100 mg of TNWs in a 100 mL reactor, add deionized water to occupy 80% of the reactor volume, and slowly add 1 mg of GO. Stir for 2 hours and place the reactor in an oven at 120 ℃ for 3 hours. Filter the obtained TNW-G1% dispersion and disperse it in water to form a 100 mL TNW-G1% solution. Vacuum filter this solution on a poly alum filter membrane to obtain the TNW-G1% membrane. After drying at 60 ℃, bake it at 120 ℃ for 12 hours. Take out the TNW-G1% membrane and calcine it in a 550 ℃ hydrogen atmosphere furnace for 4 hours to obtain the TNW-G1% membrane. Using the above method, TNW-G membranes with different GO contents were prepared, labeled as TNW-G0%, TNW-G1%, TNW-G2%, TNW-G3%, and TNW-G5%.

2.2 Performance evaluation of membrane

2.2.1 Short time filtration test of GO, GOT, and GOT/P membranes

Filter 35 mL of a 10 μmol/L direct red 80 dye solution with GO, GOT, and GOT/P25 membranes (under approximately 1 bar pressure), stop filtering after 30 minutes, collect the filtrate, and repeat each experiment three times.

2.2.2 Filtration effect test of GOT/P25 membrane

Filter with the GOT/P25 membrane under both light and no-light conditions (approximately 1 bar pressure) using 150 mL of 10 μmol/L direct red 80 solution. Collect the filtrate every 30 minutes, stopping the experiment after 3.5 hours. The direct blue 15 solution was also used for the same experiment, with the experiment stopped after 5 hours. Each experiment was repeated three times.

2.2.3 Adsorption test of GOT and P25

Add 0.2 mg of GOT to 35 mL of a 10 μmol/L direct red solution, stir for 30 minutes and 1 hour in the dark, then take samples, centrifuge, and measure the UV absorbance of the solution. The same experiment was conducted with 1.5 mg of P25. Each experiment was repeated three times.

2.2.4 Filtration effect test of TNW-G membrane

Adjust pump pressure to 0.01 MPa, filter 50 mL of a 20 mg/L direct yellow 50 dye solution with TNW-G0%, TNW-G1%, TNW-G2%, TNW-G3%, and TNW-G5% membranes respectively, record the required time, collect filtrate, and measure its UV absorbance. Each experiment was repeated three times.

2.2.5 TNW-G compound photodegradation direct yellow test

Add 100 mL of a 20 mg/L direct yellow 50 dye solution to a quartz tube, add 20 mg of TNW-G0% compound, and irradiate with 365 nm light while stirring. Take samples every 15 minutes, centrifuge, and measure the UV absorbance. The degradation effect of TNW-G0.5%, TNW-G1%, TNW-G2%, and TNW-G5% was tested by the same method.

2.3 Characterization of membrane

2.3.1 X-ray powder diffraction analysis (XRD)

The crystal structure of the sample was analyzed using a Bruker D8 Advance X-ray diffractometer. The radiation source was CuKα with $\lambda = 0.15406$ nm, operating at 40 kV and 40 mA, with a scanning step of 0.02°, scanning speed of 0.2 s/step, and a range of 5∼80°.

2.3.2 *Scanning electron microscope (SEM)*

A SU8010 field emission SEM from HITACHI, Japan, was used to characterize surface morphology and film thickness. The scanning acceleration voltage was 0.1∼30 kV, and the vacuum in the sample chamber was less than 2.7 × 10 Pa.

2.3.3 *Transmission Electron Microscope (TEM)*

The shape, size, particle size distribution, and dispersion of nanoparticles were observed using a Tecnai G2 F20 S-TWIN TEM from the Netherlands.

2.3.4 *Calculation of specific surface area (BET)*

The specific surface area of the sample was measured with a Micromeritics ASAP 2020 analyzer using N_2 static adsorption. Samples were pretreated at 300°C until the sample chamber vacuum was below 10^{-5} Torr. Using the adsorption isotherm for P/P_0 values between 0 and 0.35, BJH analysis was used for pore size distribution, and the multi-point BET method was applied to calculate the specific surface area.

2.3.5 *Thermogravimetric analysis (TG)*

A NETZSCH thermogravimetric analyzer was used for thermogravimetric analysis in an air atmosphere, with a heating rate of 5 ℃/min from 25 ℃ to 800 ℃.

2.3.6 *Total organic carbon content analysis (TOC)*

The total organic carbon content of the filtrate was determined using a TOC-VCPH analyzer.

3 Results

After inserting nanoparticles between layers, two-dimensional nano channels are disrupted, which directly affects the filtration performance of the GOT membrane loaded with particles. The compact graphene oxide sheets are partially stretched, enlarging the space between layers and enhancing solvent permeability through the GOT membrane. The water permeability of the GOT membrane was tested by filtering pure water. The results showed that the flow rate of the membrane increased. For example, the flow rate of a pure graphene oxide membrane was 27 L/hr/m^2, while the flow rate of the GOT membrane increased to 78 L/hr/m^2 (with approximately 0.2 mg of graphene oxide). Thus, water treatment capacity can be improved by enhancing filtration performance. We used Direct Red 80 (DR) solution to evaluate the filtration performance of these membranes. The results, listed in Table 3, show that when the amount of graphene oxide is the same, the GOT membrane demonstrates a higher filtration rate than the pure graphene oxide membrane due to the modified nano channels. For instance, as seen in items 2 and 5, the flow rate of the GOT membrane is about 35 L/hr/m^2, three times that of the pure graphene oxide membrane.

Considering that the GOT membrane we prepared contains TiO_2 nanoparticles, we selected the sample from Item 5 in Table 3 as a template to study its filtration performance under UV irradiation. However, as shown in Table 4 (Items 1 and 2), the retention rate of the GOT membrane for the direct red solution did not increase, which may be due to the small quantity of TiO_2 particles and their low crystallinity. Therefore, we speculate that the TiO_2 nanoparticles inserted into the GOT membrane mainly play a supporting role rather than serving as an effective photocatalytic agent. In our experiment, the amount of graphene oxide used is very low (a 0.3 mg sample contains about 0.2 mg of graphene oxide). Consequently, dye adsorption by these membranes can be almost ignored, and most of the trapped dyes remain on the surface of the GOT membranes. It can be inferred that adding a layer of photocatalyst on the surface of the membrane using photocatalysis technology could help to remove the trapped substances.

It has been reported that nanoparticles can be trapped on the surface of graphene-based filter membranes. Therefore, it is feasible to apply the same filtering method to cover a particle layer on the surface of these membranes. By filtering a dispersion containing nanoparticles (1.5 mg in 10 mL of water), we loaded the traditional TiO_2 photocatalyst (Degussa, P25) onto the surface of the GOT membrane to form a unique layered filter membrane, referred to as GOT/P25. This layered structure can be confirmed through morphological analysis. Figure 2 shows field emission scanning electron microscope images of the GOT and GOT/P25 films. Due to the low amount of the GOT film (0.2 mg of GO film), the thickness of the GOT film is very small (about 150 nm, as shown in Figures 2a and 2b), which is consistent with digital photographs. Figures 2c and 2d show typical GOT/P25 films. As seen in Figure 2c, in addition to the GOT films, an additional layer of nanoparticles (about 1 μm thick) is formed on the surface of these GOT films, indicating the formation of GOT/P25 films with a layered structure. Furthermore, it can be observed from the back of this membrane that P25 nanoparticles can hardly penetrate the GOT membrane, suggesting that the GOT filter membrane can effectively trap these particles on its surface (the pore diameter of GOT is about 3.5 nm).

Entry	Sample	Usage of GO (mg)	DR solution (10μmol/L, 35mL)	
			$flux(L \cdot h^{-1} \cdot m^{-2})$	Retention rate (%)
1	GO	0.1	14.46±0.4	79.3±0.4
2	GO	0.2	10.6±0.4	87.3±1.4
3	GO	0.5	7.7±0.3	98.6±0.3
4	GO- TiO_2	0.1	48.6±0.2	48.3±0.5
5	GO- TiO_2	0.2	35.6±0.2	58.2±0.3
6	GO- TiO_2	0.5	28.4±0.2	76.5±0.3

Table 3. Effect of GO and GOT membrane filtration on direct red

Entry	$Sample^a$	$Light^b$	DR solution (10μmol/L, 35mL)	
			$flux(L \cdot h^{-1} \cdot m^{-2})$	Retention rate (%)
1	GO- TiO_2	Off	35.6±0.2	58.2±0.3
2	GO- TiO_2	On	35.6±0.5	58.4±2.1
3	GO- $TiO_2/P25$	Off	31.8±0.3	84.7±1.3
4	GO- $TiO_2/P25$	On	28.4±0.5	93.2±2.1

[a]$Usage$ of GO sheets in these sample is about 0. 2mg. [b]$Light$ intensity is about 10 mW/cm^2. 254 nm

Table 4. Effect of GOT and GOT/P25 membranes on filtering direct red solution

Thus, it is relatively easy to control the thickness of the loading layer by simply adjusting the amount of nanoparticles. Despite the additional layer, the GOT/P25 film remains very thin, with transparency similar to that of the GOT film.

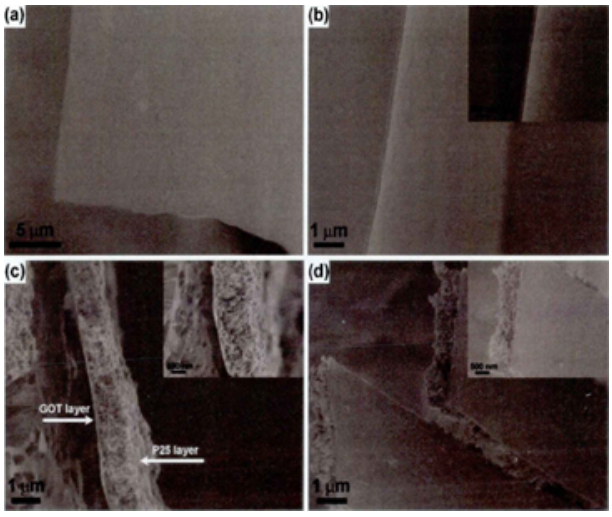

Figure 2. (a), (b) GOT and (c), (d) FESM of GOT/P25

Similarly, we explored the filtration performance of the GOT/P25 membrane by filtering a direct red dye solution, as shown in Table 5. After loading with P25, the filtration flow rate of the GOT/P25 membrane was slightly reduced, while rejection was improved compared to the GOT membrane (entries 1 and 3 in Table 4). As shown in Figures 2c and 2d, the P25 nanoparticles formed an additional layer on the GOT film. This nanoparticle layer can adsorb some dye molecules (about 11.6%) as a filter layer, which affects the filtration performance to a certain extent. Since the top layer has strong photocatalytic activity, trapped dye molecules can be removed under UV light irradiation. We also performed filtration experiments with GOT/P25 membranes under UV light irradiation (entry 4 in Table 4). We found that the retention rate was further enhanced when the direct red solution was filtered for 30 minutes, indicating that the photocatalytic degradation of pollutants contributed to the process. The P25 photocatalyst can generate reactive oxygen species, such as photogenerated holes and superoxide radicals, under UV light irradiation; these oxygen species can effectively decompose organic compounds such as the dye molecules, thereby helping to maintain the cleanliness and filtration properties of the membrane.

Entry	Sample	Light	DR solution (10μmol/L, 35mL)	
			$flux(L \cdot h^{-1} \cdot m^{-2})$	Retention rate (%)
1	GO/P25	Off	51.3±0.3	97.5±1.3
2	GO/P25	On	5.6±0.5	98.3±2.4

Table 5. Effect of GO/P25 membrane filtration of direct red dye

Figure 3 shows the XRD pattern of TiO_2 nanofibers (TNWs) after calcination at 550 ℃ in an N_2 atmosphere. It can be observed from the figure that the calcined TNWs are not anatase TiO_2 but possess the structure of $Na_yH_{2-y}Ti_nO_{2n+1} \cdot xH_2O$ or $H_2Ti_nO_{2n+1} \cdot xH_2O$ titanate, known as TiO_2-B.

Figure 4 is scanning electron microscope image of prepared TNWs. It can be seen from figure that

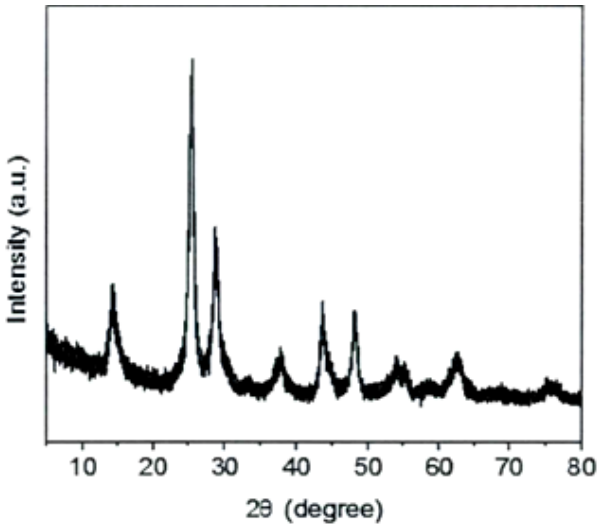

Figure 3. XRD patterns of TiO_2-B

diameter of TiO_2 nanowires is between 20 and 100 nm, and length is about several microns.

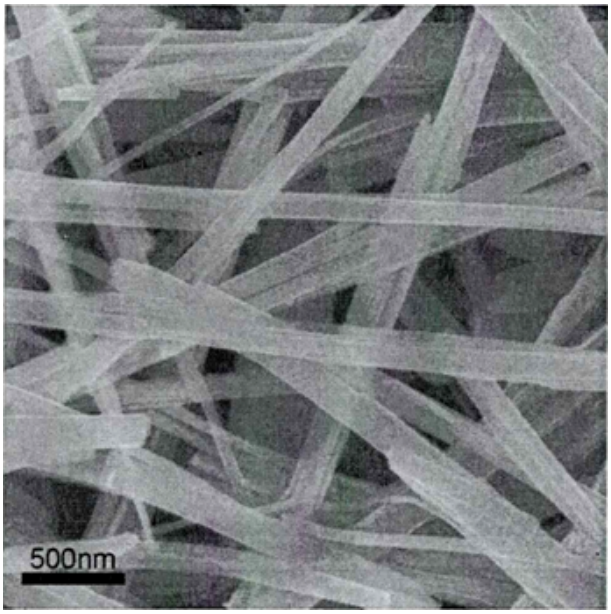

Figure 4. FESEM images of TNWS

Figure 5(a) is TEM diagram of prepared TiO_2 nanowires (TNWs), from which it can also be confirmed that diameter of TiO_2 nanowires is between 20-100 nm. Figure 5(b) is TEM diagram of composite of TiO_2 nanowires and graphene oxide prepared. It can be seen that graphene oxide sheets attach to surface of TiO_2 nanowires, but due to large graphene oxide sheets, some holes are covered.

We explored the filtration performance of the TNW-G membrane by filtering direct yellow 50, as shown in Table 6. With an increase in the amount of graphene added, the treatment capacity of the TNW-G membrane for direct yellow gradually improved, along

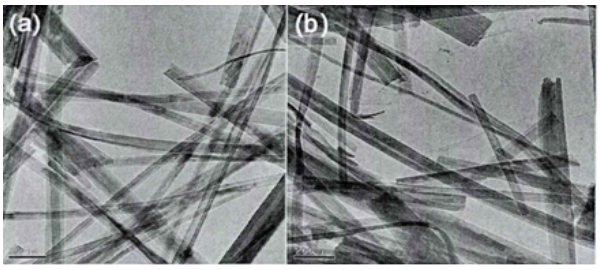

Figure 5. (a)TEM images of samples TNWs, and (b) composite of TNWs and graphene oxide

with an increase in adsorption capacity. However, the retention rate of the TNW-G membrane for direct yellow does not necessarily increase with the addition of more graphene. As the graphene content increases, the flow rate of the TNW-G membrane for filtering direct yellow gradually decreases. This is due to graphene's strong hydrophobicity, and because its distribution within the TNW-G membrane is relatively uniform, it acts as a barrier that somewhat prevents liquid penetration.

Entry	Sample	DR solution (10μmol/L, 35mL)		Adsorption rate (%)
		$flux(L \cdot h^{-1} \cdot m^{-2})$	Retention rate (%)	
1	TNW-G0%	5.5±0.5	32.4±0.5	10.7±0.3
2	TNW-G1%	5.2±0.2	39.3±0.6	19.5±0.3
3	TNW-G2%	4.3±0.2	41.05±0.5	19.5±0.2
4	TNW-G3%	3.1±0.4	50.2±0.1	26.2±0.3
5	TNW-G5%	2.3±0.3	63.2±0.6	26.3±0.3

Table 6. The effect of TNW-G membrane filtration of direct yellow dye

Figure 6 shows the N_2 adsorption-desorption isotherms and pore size distribution curves of TNW-G0% and TNW-G1% membranes. The specific surface area of the TNW-G0% membrane is 43 m^2/g, while that of the TNW-G1% membrane is 37 m^2/g. It can be seen from the figure that the pore size distribution of the TNW-G0% membrane is more concentrated than that of the TNW-G1% membrane. The pore size of the TNW-G0% membrane is primarily centered around 38 nm. The addition of graphene in the TNW-G1% membrane affects the pore size distribution of the fibers. Due to the filling effect of graphene, some of the pore sizes become smaller (around 22 nm); on the other hand, it is possible that nanowires partially assemble on the graphene, disrupting the original uniform mesoporous structure and resulting in a broader pore size distribution. Consequently, most direct yellow dye molecules can pass through the larger pores of the TNW-G membrane, leading to no significant improvement in the retention effect of the membrane.

Figure 7 shows the degradation results of direct yellow

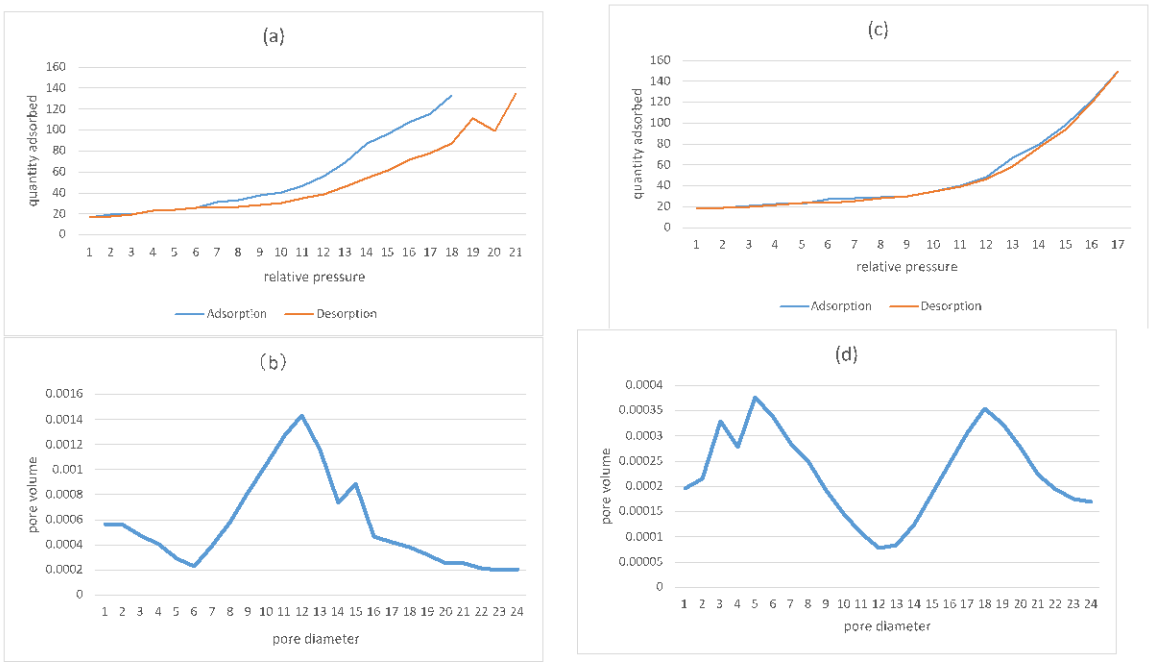

Figure 6. (a), (b) and (c), (d) are N_2 adsorption-desorption isotherms and pore size distribution curves of TNW-G0% and TNW-G1%

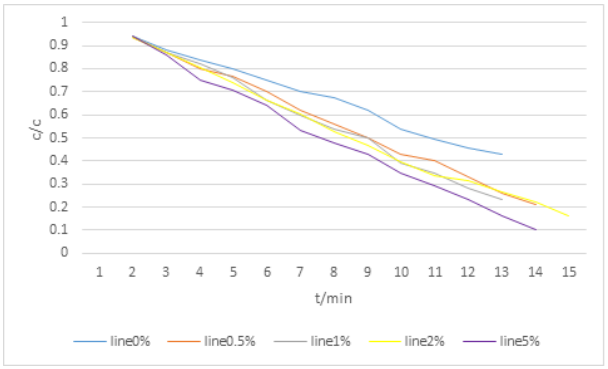

Figure 7. Degradation effect of TNW-G complexes on DY under UV light irradiation

(DY) by TNW-G complexes. As the illumination time increases, the absorbance value of the DY solution decreases. Additionally, with an increase in the amount of graphene added, the degradation effect of the composite on DY improves. When the addition ratio is 1%, the best effect is achieved. However, as the amount of graphene continues to increase beyond this point, the degradation effect worsens. This may be due to the higher amount of graphene and the darker color of the composite, which could hinder the catalyst's absorption of ultraviolet light. The experiments indicate that the composite filter membrane we prepared exhibits a certain degradation effect on direct yellow dye.

4 Discussion

Water is a precious resource, and our survival and development are closely tied to it. With the advancement of human society, the demand for water has increased, leading to a dramatic rise in water consumption. At the same time, various types of wastewater are discharged into natural water bodies, resulting in wastage and pollution, and the availability of freshwater resources is diminishing, which has severely hindered the development and progress of human society. Addressing the problem of water pollution has become urgent and essential. Research into new sewage treatment technologies, particularly environmentally-friendly options, has become a focal point for environmental protection efforts. Graphene is considered a promising photocatalyst modifier due to its high light transmittance, high electron mobility, high specific surface area, and stable chemical properties [21, 22]. Titanium dioxide/graphene materials were developed through chemical exfoliation in solution, and this experiment demonstrated a significant improvement in catalytic efficiency compared to titanium dioxide alone [23]. Cadmium sulfide/graphene materials, obtained via hydrothermal methods, have shown excellent performance in visible light catalytic oxidation [24]. Additionally, zinc oxide/graphene composites

were successfully developed, greatly enhancing photocatalytic activity for organic dye degradation [25]. Recent developments in graphene-based nano-photocatalyst materials suggest that these materials will play a crucial role in future modified photocatalyst applications, with titanium dioxide being a preferred choice for composites with graphene.

In this study, TiO_2 nanowires were reassembled by incorporating graphene oxide to create composite filter membranes. Specifically, TiO_2 nanowires with added graphene oxide were assembled by vacuum filtration to produce graphene oxide TiO_2 nanowire films, which were then reduced to obtain graphene TiO_2 nanowire films (TNW-G films). The TNW-G films prepared by these methods exhibited certain effectiveness in treating direct yellow 50 dye. Without the addition of graphene, the treatment capacity of the prepared membrane for direct yellow dye was approximately 32%. After adding 1% graphene, the treatment capacity increased to about 39%, and further increases in graphene content progressively enhanced the membrane's treatment capacity for direct yellow dye. However, as the amount of graphene increased, the membrane's adsorption capacity for direct yellow dye also grew. Comparing adsorption and filtration effects reveals that the addition of graphene primarily enhances the membrane's adsorption capacity. Additionally, photocatalysis tests on the TNW-G complex indicated that when 1% graphene was added, the TNW-G complex demonstrated the greatest capacity to degrade direct yellow. However, with higher graphene content, the degradation effect declined, possibly because the composite's darker color and high graphene concentration hinder UV light absorption by the catalyst. This suggests that the TNW-G prepared in this study possesses a certain capability for photodegradation of direct yellow dye. However, the TiO_2 nanowire membrane has a relatively fixed pore size, which limits its ability to selectively separate pollutants. By incorporating graphene as a filler, leveraging the planar two-dimensional structure of graphene sheets, it is expected that graphene sheets can partially block the pore size of TiO_2 nanowire membranes, thereby improving separation performance. Experimental results reveal both the effects and limitations of adding graphene to fiber filter membranes. In the future, the separation effectiveness of fiber filter membranes could be enhanced by adjusting the physical and chemical properties of the graphene sheets added, and the photocatalytic degradation capability of composite filter membranes containing graphene will continue to be explored.

Data Availability

The experimental data used to support the findings of this study are available from the corresponding author upon request.

Conflicts of Interest

The authors declared that they have no conflicts of interest regarding this work.

Funding Statement

This work was supported by Key Research and Development Program of Lianyungang(SF2334).

References

[1] Shuang, S., Lv, R., Cui, X., Xie, Z., Zheng, J., & Zhang, Z. (2018). Efficient photocatalysis with graphene oxide/Ag/Ag 2 S–TiO 2 nanocomposites under visible light irradiation. *RSC Advances, 8*(11), 5784-5791.

[2] Alothman, A. A., El-Naggar, M. E., Afifi, M., Mushab, M. S. S., Sillanpää, M., & Kenawy, E. R. (2022). Optimizing Graphene Oxide Encapsulated TiO 2 and Hydroxyapatite; Structure and Biological Response. *Journal of Inorganic and Organometallic Polymers and Materials*, 1-13.

[3] Ahmad, H. H., & Alahmad, W. (2021). Modeling the removal of methylene blue dye using a graphene oxide/TiO2/SiO2 nanocomposite under sunlight irradiation by intelligent system. *Open Chemistry, 19*(1), 157-173.

[4] Vajedi, F., & Dehghani, H. (2019). The characterization of TiO2-reduced graphene oxide nanocomposites and their performance in electrochemical determination for removing heavy metals ions of cadmium (II), lead (II) and copper (II). *Materials Science and Engineering: B*, 243, 189-198.

[5] Abasali Karaj Abad, Z., Nemati, A., Malek Khachatourian, A., & Golmohammad, M. (2020). The effect of pre-reduction of graphene oxide on the electrochemical performance of rGO-TiO2 nanocomposite. *Iranian Journal of Materials Science and Engineering, 17*(4), 55-61.

[6] Kumari, S., Shekhar, A., & Pathak, D. D. (2019). Correction: Graphene oxide–TiO 2 composite: an efficient heterogeneous catalyst for the green synthesis of pyrazoles and pyridines. *New Journal of Chemistry, 43*(42), 16767-16768.

[7] Gohr, M. S., Hafez, H. S., Saif, M. M., Soliman, H., & Abdel-Mottaleb, M. S. A. (2020). Facile hydrothermal synthesis of Sm and Eu doped TiO2/graphene oxide nanocomposites for photocatalytic applications. *Egyptian Journal of Chemistry, 63*(4), 1359-1382.

[8] Vajedi, F., & Dehghani, H. (2019). The characterization of TiO2-reduced graphene oxide nanocomposites and their performance in electrochemical determination for removing heavy metals ions of cadmium(II), lead(II) and copper(II). Materials Science and Engineering, 243(APR.), 189-198.

[9] Pei, P., Whitwick, M. B., Kureshi, S., Cannon, M., Quan, G., & Kjeang, E. (2020). Hydrogen storage mechanism in transition metal decorated graphene oxide: the symbiotic effect of oxygen groups and high layer spacing. *International Journal of Hydrogen Energy, 45*(11), 6713-6726.

[10] Baek, S., Joo, S. H., Su, C., & Toborek, M. (2019). Antibacterial effects of graphene-and carbon-nanotube-based nanohybrids on Escherichia coli: Implications for treating multidrug-resistant bacteria. *Journal of Environmental Management, 247*, 214-223.

[11] Vinothkannan, M., Kim, A. R., & Yoo, D. J. (2018). Sulfonated graphene oxide/Nafion composite membranes for high temperature and low humidity proton exchange membrane fuel cells. *RSC Advances, 8*(14), 7494-7508.

[12] Shi, K., Wang, Z., Xu, H., Xu, Z., Zhang, X., Zhao, X., ... & Liu, Y. (2018). Complementary resistive switching observed in graphene oxide-based memory device. *IEEE Electron Device Letters, 39*(4), 488-491.

[13] Farooqui, U. R., Ahmad, A. L., & Hamid, N. A. (2018). Graphene oxide: A promising membrane material for fuel cells. *Renewable and Sustainable Energy Reviews, 82*, 714-733.

[14] Priya, T., Dhanalakshmi, N., Thennarasu, S., & Thinakaran, N. (2018). A novel voltammetric sensor for the simultaneous detection of Cd2+ and Pb2+ using graphene oxide/κ-carrageenan/l-cysteine nanocomposite. *Carbohydrate Polymers, 182*, 199-206.

[15] Avornyo, A., & Chrysikopoulos, C. V. (2024). Applications of graphene oxide (GO) in oily wastewater treatment: Recent developments, challenges, and opportunities. *Journal of Environmental Management, 353*, 120178.

[16] Lu, H. Y., Liu, W. F., Qin, L., & Liu, X. G. (2024). The use of carbon-based particle electrodes in three-dimensional electrode reactors for wastewater treatment. *New Carbon Materials, 39*(5), 973-991.

[17] Ibrahim, A., & Nazeer, S. On the Various Energy Forms of the Join of Complete Graphs. *Journal of Combinatorial Mathematics and Combinatorial Computing, 122*, 185-195.

[18] Altay, A., & Mirici, İ. H. (2024). Efl Instructors' Implementations of 21st Century Skills in Their Classes. *International Journal for Housing Science and Its Applications, 45*(2), 37-46.

[19] Li, D. The Comprehensive Training Effect of Translation Ability of College English Majors Based on Machine Learning. *Journal of Combinatorial Mathematics and Combinatorial Computing, 120*, 399-410.

[20] Wu, Y. Exploration of the Integration and Application of the Modern New Chinese Style Interior Design. *International Journal for Housing Science and Its Applications, 45*, 28-36.

[21] Chen, P. Research on Business English Approaches from the Perspective of Cross-Cultural Communication Competence. *International Journal for Housing Science and Its Applications, 45*, 13-22.

[22] Sanchez, S. N. B., da Silveira Salla, J., Cesconeto, L. P., da Rocha, G. L., Virmond, E., & Moreira, R. D. F. P. M. (2024). Synthesis of multi-layer graphene oxide from HCl-treated coke and Brazilian coals by sulfuric acid thermal exfoliation and ozone oxidation. *Heliyon, 10*(9), e30546.

[23] Parandi, E., Safaripour, M., Mosleh, N., Saidi, M., Nodeh, H. R., Oryani, B., & Rezania, S. (2023). Lipase enzyme immobilized over magnetic titanium graphene oxide as catalyst for biodiesel synthesis from waste cooking oil. *Biomass and Bioenergy, 173*, 106794.

[24] Subramanian, N., Perumal, T., Mangesh, V. L., Chinnadurai, R., Sakthinathan, S., Chiu, T. W., ... & Madhavan, J. (2023). Future Perspectives on Zeolite/Graphene Oxide Composite Synthesis and Applications. *Energy & Fuels, 37*(22), 17013-17051.

[25] Sanchez, S. N. B., Spaolonzi, M. P., Cesconeto, L. P., Souza, L., Virmond, E., Vieira, M. G. A., ... & Moreira, R. D. F. P. M. (2024). Adsorption of Ciprofloxacin on Graphene Oxide-Based Adsorbents: Synthesis, Characterization and DFT Calculations. *Water, Air, & Soil Pollution, 235*(6), 417.